Photopic Negative Response Recorded with RET*eval*™ System in Eyes with Optic Nerve Disorders

Tsutomu Yamashita (tsutomu-y@mw.kawasaki-m.ac.jp)
Kawasaki University of Medical Welfare
Kumiko Kato
Mie University Graduate School of Medicine
Mineo Kondo
Mie University Graduate School of Medicine
Atsushi Miki
Kawasaki University of Medical Welfare
Syunsuke Araki
Kawasaki Medical School
Katsutoshi Goto
Kawasaki Medical School
Yoshiaki Ieki
Kawasaki Medical School
Junichi Kiryu
Kawasaki Medical School

Research Article

Keywords: photopic negative response, electroretinography, RETeval system, optic nerve disorder, circumpapillary retinal nerve fiber layer thickness.

Posted Date: February 10th, 2022

DOI: https://doi.org/10.21203/rs.3.rs-1325636/v1

Abstract

Background: Electroretinography (ERG) is used to evaluate the physiological status of the retina and optic nerve. The purpose of this study was to determine the usefulness of ERGs recorded with the RET*eval* system in diagnosing optic nerve diseases.

Subjects and methods: Forty-eight patients with optic nerve disorders, including optic neuritis, ischemic optic neuropathy, traumatic optic neuropathy, and dominant optic atrophy, and 36 normal control subjects were studied. The amplitudes of the photopic negative response (PhNR) were recorded with the RET*eval* system without mydriasis. The circumpapillary retinal nerve fiber layer thickness (cpRNFLT) was determined by optical coherence tomography (OCT). The significance of the correlations between the PhNR and cpRNFLT parameters were determined, and the receiver operating curve (ROC) analyses were performed for the PhNR and cpRNFLT.

Results: Patients with optic nerve disorders had a significantly smaller PhNRs compared to the control subjects (P=0.001). The ROC analyses indicated that both PhNR and cpRNFLT had comparable diagnostic abilities of detecting optic nerve disorders with PhNR at 0.857 and cpRNFLT at 0.764.

Conclusion: The PhNR components recorded with the RET*eval* system have comparable diagnostic ability as the cpRNFLT in diagnosing optic nerve disorders.

Introduction

The photopic negative response (PhNR) is a component of the full-field electroretinogram (ERG), and it is a slow negative wave that follows the b-wave. It originates primarily from the retinal ganglion cells and their axons[1–3]. The amplitude of the PhNR is reduced in disorders that affect the innermost retina[4], and the results of earlier studies have shown that it is reduced in glaucoma[5,6], retinal vascular diseases[7], and optic nerve atrophy[8–10]. Thus, the PhNR has been used to help in the diagnosis of retinal nerve fiber disorders. However, recording and analyzing the PhNR using conventional ERG recording systems can be time consuming and the examination procedures are somewhat invasive.

The recently developed RET*eval* system (LKC Technologies Inc., Gaithersburg, MD, USA) allows clinicians to record ERGs quickly and less invasively. The RET*eval* system uses seal-type skin electrodes which allows the recording of ERGs from adults and children relatively simply. It has been reported that the RET*eval* system was as helpful as the conventional ERG recording systems in diagnosing and evaluating ophthalmic diseases such as diabetic retinopathy[11–13] and retinal vein occlusions[14,15]. The RET*eval* system can record not only the standard full-field ERGs conforming to the International Society for Clinical Electrophysiology of Vision (ISCEV) guidelines but also the PhNRs[16,17]. Although the reliability of the PhNRs recorded with skin electrodes is a concern for many doctors, it has been reported that PhNRs recorded with skin electrodes are as useful in diagnosing diseases as those recorded with the contact lens-type of electrodes[16].

Gotoh et al studied the correlation between the PhNR recorded with a conventional ERG recording system and retinal nerve fiber layer thickness (RNFLT) measured by optical coherence tomography (OCT) in 10 patients with optic nerve atrophy[8]. They reported that the two parameters were highly correlated, and they stated that the PhNR can be used to evaluate the function of retinal ganglion cells and their axons in eyes with optic nerve atrophy. However, there have not been any studies that determined the correlations between the PhNR and the RNFLT in the acute phase of optic nerve disorders including optic neuritis (ON) and ischemic optic neuropathy (ION). In addition, there have not been any studies that determined whether the PhNR recorded by the RET*eval* system can be used to diagnose optic nerve disorders.

Thus, the purpose of this study was to determine whether PhNRs recorded with the RET*eval* system and circumpapillary RNFLT (cpRNFLT) obtained by OCT are significantly correlated in eyes with optic nerve disorders, and to determine whether PhNRs can be used in diagnosing optic nerve disorders.

Results

Clinical Characteristic of Subjects

The demographics of the patients are shown in Table 1. Forty-eight eyes of 48 patients with optic nerve disorders were classified according to the etiology of the disorder. There were 17 eyes with inflammation (acute phase, 6 eyes; chronic phase, 11 eyes). Seven of the 11 patients at the chronic phase received steroid pulse therapy. There were 19 eyes with ischemia with 7 at the acute phase and 12 eyes at the chronic phase. There were 6 eyes with traumatic optic neuropathy (TON), and 6 eyes with dominant optic atrophy. The 13 eyes with ON and ION were placed in the acute ON/ION group and 23 eyes were placed in the chronic ON/ION group.

Table 1
Demographics of Subjects

	Control	Overall optic nerve disorders	Acute ON/ION	Chronic ON/ION	TON/DOA
Subject	36	48	13	23	12
Age (years)	59.7 ± 18.2	55.7 ± 19.1	59.0 ± 15.3	61.4 ± 15.2	41.3 ± 23.2
P-value		0.480	0.997	0.978	0.003*
Sex (men/women)	14 / 22	21 / 27	5 / 8	7 / 16	9 / 3
P-value		0.823	1.000	0.585	0.046*
Refractive error	-0.88 ± 2.69	-0.61 ± 2.13	0.23 ± 1.78	0.68 ± 0.54	-1.50 ± 1.86
P-value		0.649	0.371	0.965	0.798

The mean interval from the onset of the symptoms and signs of optic nerve disorder to the initial examination was 0.68 ± 0.62 months (range, 0-2.3 months) for the acute ON and ION group and 6.63 ± 6.84 months (range, 3.0-32.3 months) for the chronic ON and ION group. The mean interval from the onset of the symptoms to the initial examination was 3.4 years for the TON (range, 3.0 months to 8.6 years).

The mean age of all the patients with optic nerve disorders was 55.7 ± 19.1 years (range, 9 to 87 years), and 21 were men and 27 were women. The data of 36 eyes of 36 of age-matched normal subjects were analyzed in the same way and served as controls. The mean age of the control subjects was 59.7 ± 18.2 years (range, 26 to 87 years) and included 14 men and 22 women. There was no significant difference in the age and sex distribution between the patients with optic nerve disorders and controls ($P = 0.480$, $P = 0.823$, respectively).

The characteristics of the amplitudes of P_{72}, P_{min}, P_{ratio}, and W_{ratio} of the PhNR, and the a- and b-waves of the ERGs of the eyes with optic nerve disorders and the normal control group are presented in Table 2. In the optic nerve disorders groups, the PhNRs were significantly smaller than that of the normal control group. The a-wave amplitude was significantly larger in the acute ON and ION group than the normal control group ($P = 0.019$). There was no significant difference in the amplitudes of the b-wave between the normal control group and optic nerve disorders group.

Table 2
ERGs and OCT for each group.

	Control	Overall optic nerve disorders	Acute ON/ION	Chronic ON/ION	TON/DOA
a-wave amplitude (μV)	-3.75 ± 1.93	-4.81 ± 2.47	-5.76 ± 2.71	-4.73 ± 2.09	-3.95 ± 2.75
P-value		0.053	0.019*	0.266	0.990
b-wave amplitude (μV)	19.44 ± 5.89	21.10 ± 7.08	24.05 ± 7.54	21.26 ± 7.03	17.62 ± 5.45
P-value		0.305	0.082	0.624	0.762
P_{72} (μV)	-4.43 ± 2.28	-1.57 ± 2.43	-2.34 ± 2.16	-1.62 ± 2.38	-0.64 ± 2.68
P-value		0.001*	0.022*	0.001*	0.001*
P_{min} (μV)	-5.35 ± 2.30	-2.70 ± 2.50	-3.67 ± 3.00	-2.41 ± 2.26	-2.22 ± 2.25
P-value		0.001*	0.093	0.001*	0.001*
P_{ratio}	0.30 ± 0.15	0.09 ± 0.16	0.14 ± 0.13	0.09 ± 0.14	0.05 ± 0.21
P-value		0.005*	0.005*	0.001*	0.001*
W_{ratio}	1.09 ± 0.14	0.90 ± 0.11	0.92 ± 0.13	0.88 ± 0.09	0.91 ± 0.12
P-value		0.001*	0.001*	0.001*	0.001*
cpRNFLT (μm)	102.7 ± 9.9	91.8 ± 46.7	151.4 ± 51.2	76.0 ± 12.2	69.5 ± 11.6
P-value		0.001*	0.001*	0.001*	0.001*
GCCT (μm)	92.7± 6.6	73.8 ± 14.0	91.1± 10.6	70.8 ± 9.9	66.3 ± 6.6
P-value		0.001*	0.904	0.001*	0.001*

The cpRNFLT was reduced significantly in the patients with optic nerve disorders compared with that of the normal control group ($P = 0.001$). The GCCT was reduced significantly in the chronic ON and ION groups and in the TON and DOA groups ($P = 0.001$), but there was no significant difference in patients with acute ON and ION ($P = 0.904$).

Fundus photographs and PhNRs of representative cases of optic nerve disorders and control group are shown in Figure 1. In the control group, full-field ERGs showed a negative wave at 72 msec (red arrow), but in the optic nerve disorders groups, the negative wave after the b-wave was considerably smaller.

Correlation between PhNRs and cpRNFLT and ganglion cell complex thickness in eyes with optic nerve disorders

The correlations between the different components of the PhNRs and the cpRNFLT and the ganglion cell complex thickness (GCCT) are shown in Table 3. The cpRNFLT was weakly but significantly correlated with the P_{72}, P_{min}, and P_{ratio} amplitudes in all cases of optic nerve disorders (r = -0.356, P = 0.013; r = -0.334, P = 0.020; and r = 0.299, P = 0.039, respectively). In the acute ON/ION eyes, the cpRNFLT was weakly but significantly correlated with the W_{ratio} (r = -0.553, P = 0.049), but the cpRNFLT was not significantly correlated with the PhNR components in the chronic ON/ION eyes. In the TON/DOA group, the cpRNFLT was significantly correlated with the P_{min} and the W_{ratio} (r = -0.720, P = 0.008; r = 0.650, P = 0.022; respectively). The correlation between the PhNRs and the GCCT was not significant.

Table 3. Univariate analysis between PhNRs and cpRNFLT, GCCT in Optic Nerve Disorders.

Variables	Variables	Overall optic nerve disorders		Acute ON/ION		Chronic ON/ION		TON/DOA	
		r	*P*-value	*r*	*P*-value	r	*P*-value	r	*P*-value
cpRNFLT	P_{72}	-0.356	0.013*	0.621	0.024*	-0.376	0.077	-0.336	0.286
	P_{min}	-0.334	0.020*	0.473	0.103	-0.324	0.131	-0.720	0.008*
	P_{ratio}	0.299	0.039*	-0.566	0.044*	0.228	0.295	0.455	0.138
	W_{ratio}	0.170	0.247	-0.553	0.049*	0.168	0.443	0.650	0.022*
GCCT	P_{72}	-0.194	0.187	0.401	0.174	-0.044	0.843	-0.077	0.812
	P_{min}	-0.134	0.365	0.247	0.415	0.027	0.601	-0.266	0.404
	P_{ratio}	0.119	0.419	-0.324	0.280	-0.115	0.902	0.056	0.863
	W_{ratio}	0.005	0.975	-0.374	0.208	-0.042	0.849	0.070	0.829

cpRNFLT, circumpapillary retinal nerve fiber layer thickness; GCCT, ganglion cell complex thickness.

ON, optic neuritis; ION, ischemic optic neuropathy; TON, traumatic optic neuropathy; DOA, dominant optic atrophy.

*P<0.05 was considered significant.

A scatter plot of the W_{ratio} and the cpRNFLT is shown in Figure 2. There was no significant correlation between the W_{ratio} and cpRNFLT for the optic nerve disorders grouped together (r = 0.170, P = 0.247). However, there was a significant negative correlation between the W_{ratio} and cpRNFLT in eyes at the acute ON and ION phase (r = -0.553, P = 0.049) but there was no significant correlation in the chronic ON and ION phase (r = 0.168; P = 0.443). There was a significant positive correlation between the W_{ratio} and cpRNFLT in the TON/DOA group (r = 0.650; P = 0.022).

Receiver Operating Characteristic Curve Analyses of Diagnostic Performance in Optic Nerve Disorders

We examined whether the different components of the PhNR recorded with the RET*eval* system can be used to differentiate eyes with from the eyes without optic nerve disorders using the receiver operating characteristic (ROC) curve (Figure 3).

The AUCs for discriminating optic nerve are shown in Table 4. When the AUCs were calculated for all subjects, the AUC was 0.857 for the W_{ratio}, 0.764 for the cpRNFLT, and 0.853 for the GCCT. The AUCs for P_{72} was 0.792, that for P_{min} was 0.670, and that for the P_{ratio} was 0.836 for all subjects (data not shown in Table 4.). The AUCs using P_{72} and the P_{ratio} were comparable to the AUC using the W_{ratio}. The sensitivity and specificity in detecting overall optic nerve disorders were 75% and 83.3% for the W_{ratio} and 75% and 91.7% for the cpRNFLT.

Table 4. Comparison of W_{ratio} and OCT sensitivities, specificity and AUCs in Optic Nerve Disorders.

	Overall			Control + Acute ON/ION			Control + Chronic ON/ION			Control + TON/DOA		
	AUC	Sensitivity (%)	Specificity (%)	AUC	Sensitivity (%)	Specificity (%)	AUC	Sensitivity (%)	Specificity (%)	AUC	Sensitivity (%)	Specificity (%)
W_{ratio}	0.857	75.0	83.3	0.810	76.9	75.0	0.877	82.6	80.6	0.829	83.3	72.2
cpRNFLT	0.764	75.0	91.7	0.789	69.2	100	0.935	95.7	88.9	0.995	100	97.2
GCCT	0.853	81.3	80.1	0.567	53.9	69.4	0.920	91.3	91.7	0.998	100	97.2

cpRNFLT, circumpapillary retinal nerve fiber layer thickness; GCCT, ganglion cell complex thickness; AUC, area under the curve.

ON, optic neuritis; ION, ischemic optic neuropathy; TON, traumatic optic neuropathy; DOA, dominant optic atrophy.

Next, we analyzed ability of each PhNR component to detect optic nerve disorders by classifying the cases into those with acute ON/ION, chronic ON/ION, and TON/DOA. When the cpRNFLT was used, the diagnostic ability was higher when the optic nerve disorders were classified into each group than when analyzed overall. In addition, the sensitivity and specificity of the diagnosis had higher values. On the other hand, when the W_{ratio} was used, there was no difference in the diagnostic accuracy; the sensitivity and specificity in diagnosing optic nerve disorders regardless of the classification of the patients.

Finally, we performed ROC analysis using the GCCT and found that the diagnostic ability of the GCCT was equal to the cpRNFLT and the W_{ratio} in the chronic ON/ION and TON/DOA eyes, but it was low at 0.567 in the acute ON/ION eyes.

Discussion

Our results showed that the amplitudes of the different parameters of the PhNR in patients with optic nerve disorders were reduced significantly to 30-80% of the normal control subjects. The ROC analyses showed that the diagnosing of optic nerve disorders with the different PhNR components was comparable to that of the diagnosing with the cpRNFLT. This suggests that recording PhNRs with the RETeval system may be a useful examination to evaluate retinal ganglion cell function in eyes with optic nerve disorders.

There are a variety of diseases that can cause abnormalities in the retinal ganglion cells including ischemia, degenerative changes, trauma, toxicity, and nutritional abnormalities. Many studies have evaluated the changes of the RNFLT in these diseases using OCT but relatively few studies have used electrophysiological tests, such as visual evoked potentials, pattern ERGs, and PhNR, to evaluate the functional changes.

The significant correlation between the PhNR and cpRNFLT has been reported in healthy subjects[18], glaucoma patients[3,19], and patients with optic nerve atrophy[8]. In our study, the scatter plots of the cpRNFLT and W_{ratio} for all of the optic nerve disorders were not significantly correlated (Figure 2, upper left), and the P_{72}, P_{min}, and P_{ratio} had only a weak correlation with the cpRNFLT (Table 3). This was because the cpRNFLT is larger at the acute ON/ION (Figure 2B) and smaller at the chronic phase of ON/ION (Figure 2B). On the other hand, the PhNR is different in that it is uniformly smaller whether at the acute ON/ION or chronic ON/ION phases. Thus, the lower variability in the cpRNFLT could be contributing to the lack of significant correlations between the cpRNFLT and PhNRs in all of the optic nerve disorders.

The question then arises as to why we did not find a significant correlation between cpRNFLT and W_{ratio} in the eyes with chronic ON/ION while a significant correlation was found in the acute ON/ION. The results showed that the standard deviation of the cpRNFLT in the acute ON/ION was large at 44 μm and it was 12.9 μm in the chronic ON/ION (Table 2). Thus, the cpRNFLT had less variability in the chronic phase of ON/ION. We suggest that the lower variability in the cpRNFLT may be the reason for the lack of significant correlations between the cpRNFLT and the W_{ratio} in the chronic phase of ON/ION.

There was a significant positive correlation between the W_{ratio} and cpRNFLT in the eyes with TON/DOA. TON, which can be cause by blunt trauma to the optic nerve, has been reported to lead to a thinning of the cpRNFLT which progresses slowly[20]. DOA is a progressive atrophy of the optic nerve caused by degeneration of the retinal ganglion cells[21]. A high correlation between the W_{ratio} and cpRNFLT in this group was probably due to the thinning of the cpRNFLT and the simultaneous decrease of the W_{ratio} with the degeneration of the retinal ganglion cells.

Our results showed that the correlation between the PhNRs and GCCT was not significant. This may be because there were no significant changes in the GCCT in the acute ON/ION phase compared to the normal group, and there was a significant thinning of GCCT in the chronic ON/ION and TON/DOA (Table 2). We suggest that this was because the anatomical abnormalities in the ganglion cell complex progress with a time lag from the onset of optic nerve injury. We believe that this can explain why the GCCT was not significantly correlated with the PhNRs.

There have been several studies that evaluated the diagnostic abilities of the PhNR in detecting glaucoma. A study on nonhuman primate of glaucoma reported that the AUC for the diagnostic ability of the PhNR in detecting glaucoma was 0.90[22]. In studies on glaucoma patients, the AUC was reported to be 0.60~0.80[6,23–25]. In our study, the AUC for diagnosing all of the cases of optic nerve disorders was 0.85 which is comparable to previous reports in glaucoma patients.

Reports on the sensitivity and specificity for the diagnostic abilities of PhNR in glaucoma patients have stated that the sensitivity ranged 53.3-76.7% and the specificity ranged 80-90%[19]. In our study of optic nerve disorders, the sensitivity ranged 76.9%-83.3% and the specificity ranged 72.2%-80.6%. The sensitivity tended to be slightly higher than the study in glaucoma patients. We believe that the sensitivity and specificity in this study of optic nerve disorders were not poorer than the results obtained in studies of glaucoma patients.

Then, the question arises as to which is better in diagnosing optic nerve disorders, the cpRNFLT or the PhNR? A study that analyzed the diagnostic performance of PhNR and cpRNFLT in glaucoma patients reported that the diagnostic abilities of these parameters were comparable[19]. Although no study has analyzed the diagnostic abilities of both PhNR and cpRNFLT in patients with optic nerve disorders, a study that analyzed the diagnostic abilities of optic nerve disorders using cpRNFLT reported that the sensitivity and specificity were 72% and 91% respectively[26]. The sensitivity and specificity of the W_{ratio} for diagnosing optic nerve disorder was 75.0% and 83.3% respectively in our study. These values are comparable to that of the earlier study using cpRNFLT[26]. Therefore, we suggest that the diagnostic abilities of PhNR in optic nerve disorders are comparable to that of cpRNFLT. Considering that the diagnostic abilities of PhNR is not inferior to that of cpRNFLT, and the interpretation of PhNR is easier because the PhNR becomes uniformly smaller than that of the normal control subjects regardless of the interval since the onset of optic nerve disorders, we believe that using both the cpRNFLT and PhNR will enable clinicians to diagnose optic nerve disorders more accurately.

Finally, the amplitude of a-wave was significantly larger in the acute ON/ION than that of the control group. A study that recorded PhNR from patients with multiple sclerosis who developed ON reported that the amplitude of the a-wave was not significantly different from that of the control group[9]. The increase in the a-wave amplitude may be limited to the very early stages of ON, it will be necessary to record PhNR from a larger number of subjects with ON during the course of the disease then determine whether the increased a-wave amplitude of PhNR is significant.

There are several limitations in this study. First, the number of patients in each group was small when classified by stage and etiology. That was because even though optic nerve disorders are relatively common in daily clinical practice, there were few cases that met all the inclusion criteria. We plan to continue our research and analyze more subjects with optic nerve disorders. The second limitation was that the PhNRs were recorded without mydriasis as the ISCEV guideline recommended. Although RET*eval* system delivers a stimulus with constant retinal illuminance by adjusting the luminance to compensate for changes of pupil size, a study that analyzed factors affecting PhNRs recorded with RET*eval* system reported that there was a significant, although weak, correlation between PhNRs and pupillary area in a univariate analysis[18]. However, this correlation was not observed in multivariable analyses, and we believe that the effect of pupil area on PhNRs would not have significant impact on the results of this study. The third limitation was that this study was a cross-sectional study, and we did not evaluate the changes in PhNR during the acute and chronic phases in the same patients with ON and ION. We need to perform a longitudinal study on eyes with ON and ION while performing ERG to use PhNR as diagnostic tool in clinical practice.

In conclusion, the amplitudes of the PhNR recorded with the RET*eval* system are highly correlated with cpRNFLT in patients with acute phase of ON/ION, and optic atrophy induced by hereditary disease and trauma. We conclude that the different components of the PhNRs are as useful as the OCT for diagnosing optic nerve diseases. PhNR is a parameter that is easy to interpret because it becomes uniformly lower in patients with optic nerve disorders, and we recommend the concomitant use of OCT and PhNR to improve the diagnosis of optic nerve disorders.

Methods

Study design

This was a retrospective, single center study conducted at the Kawasaki Medical School Hospital between July 2017 and April 2019. The Medical Ethics Committee of the Kawasaki Medical School Hospital approved the procedures used (No. 3296), and the procedures conformed to the tenets of the Declaration of Helsinki of the World Medical Association. After the nature and possible consequences of the study were explained, a signed written informed consent was obtained from each of the participating patients.

Participants

The optic nerve disorders were diagnosed by a neuro-ophthalmology specialist (AM) based on the clinical findings. The participants underwent comprehensive ophthalmologic examinations including measurements of the best-corrected visual acuity (BCVA) and intraocular pressure, and slit-lamp biomicroscopy, color fundus photography, optical coherence tomography, and kinetic or static visual field perimetry. Patients were excluded if they had a systemic neurological disease or history of a retinal disease including diabetic or hypertensive retinopathy and a history of eye surgery. In patients with bilateral optic neuropathy, one eye was selected at random for the statistical analyses. In addition, 36 age and sex matched healthy subjects were studied in the same way and served as controls. Only one eye was randomly selected in the control group. The ON and ION were classified into the acute phase and chronic phase according to past reports[27–29]. The acute ON/ION was defined as having a swelling of the optic nerve that was evident ophthalmoscopically and was detected within three months of the onset of symptoms and signs. Chronic ON/ION was defined when more than three months had passed since the onset of symptoms and the swelling of the optic disc had disappeared. Patients with traumatic optic neuropathy (TON) or dominant optic atrophy (DOA) were placed in the TON/DOA group. The acute ON/ION, the chronic ON/ION, and the TON/DOA groups were collectively referred to as overall optic nerve disorder.

PhNR recording by RET eval system

Full-field PhNRs were recorded with the RET*eval* system from all patients and controls with natural pupils under room lighting. The PhNR recordings were performed by experienced ophthalmic technicians (SA, KG). After cleaning the skin with 70% isopropyl alcohol swabs, the sensor strip skin electrode array (Sensor Strip; LKC Technologies Inc., Gaithersburg, MD, USA) was carefully placed 2 mm below the lower eyelid on the orbital rim of both eyes and connected to the sensor strip lead. This strip included the active, reference, and ground electrodes in a single adhesive tape. The contralateral eye was covered during the recordings. A mini Ganzfeld dome was placed in front of the eye, and the eye was stimulated with red flashes (621 nm, 38 Td·s) on a steady blue background (470 nm, 380 Td) which saturated the rod and isolated the cone responses. The stimulus frequency was 3.4 Hz, and 200 responses were averaged for each recording to increase the signal-to-noise ratio. The patients were instructed to fixate a fixation point within the dome, and the patient's fixation was monitored by an infrared camera. During the stimulation, the pupil size (mm^2) was automatically measured in real-time, and the stimulus flash luminance (cd-s/m^2) was continuously adjusted to maintain a constant flash retinal illuminance (Td-s) by the following equation:

Photopic flash retinal illuminance (Td-s) = Photopic flash luminance (cd-s/m^2) × pupillary area (mm^2).

Analyses of ERGs

The methods used to measure each ERG component are shown in Figure 4. The a-wave amplitude was measured from the pre-stimulus baseline to the first negative trough, and the b-wave amplitude was measured from pre-stimulus baseline to the positive peak. The PhNR amplitude was measured at two points; at 72 ms from the stimulus onset and the second was measured at the negative trough immediately following the b-wave between 55 ms and 100 ms. The first amplitude was measured from the pre-stimulus baseline to the negative trough at 72 msec after the stimulus onset (P_{72}), and the second amplitude was measured from the baseline to the negative trough after the b-wave (P_{min}). The ratio of PhNR amplitude at 72 ms to b-wave peak was designated as the P_{ratio}

(P_{72} voltage/b-wave voltage)[17]. The ratio of the b-wave peak voltage to the PhNR trough voltage to b-wave amplitude was designated as the W_{ratio} (b-wave voltage – Pmin voltage)/(b-wave voltage – a-wave voltage)[30]. We used the W_{ratio} in most of the statistical analyses because it has been reported to have the lowest inter-individual, inter-session, and inter-ocular variations[30]. The PhNR data were analyzed by specialists of visual electrophysiology (MK, KK). Cases were excluded if the ERGs could not be recorded due to significant vision loss or the ERGs could not be analyzed due to significant noise.

Protocol for OCT examinations

OCT examinations were performed by experienced ophthalmic technicians (SA, KG). The OCT images were recorded with the RTVue-100 SD-OCT (RTVue-100, Optovue, Inc., Fremont, CA, USA), which can acquire 26,000 A-scans/sec and had a 5-μm depth resolution. The Versuib 4.0 software of RTVue-100 was used for data acquisition. The cpRNFLT was determined using the nerve head map 4-mm protocol in the three-dimensional baseline mode in which data along a 3.45-mm diameter circle around the optic disc were recalculated with a map created from en face images that used 6 circular scans ranging from 2.5 to 4.0 mm in diameter (587 or 775 A scans each). The scans were centered on the optic disc and consisted of data from 12 linear radial scans (3.4-mm length, 452 A scans each). This scan protocol recorded 9510 A scans/0.39 seconds. The cpRNFLT map was generated from the three-dimensional video images after defining the optic disc margin and anchoring points of the retinal pigmented epithelium by the examiners.

The ganglion cell complex (GCC) protocol was used to obtain the macular measurements. This protocol consisted of 1 horizontal line scan of 7 mm in length (467 A scans) and 15 vertical line scans 7 mm in length (each 400 A scans) at 0.5-mm intervals. The center of the GCC scan was shifted 0.75 mm temporally to improve the sampling of the temporal periphery. This scan configuration recorded 14810 A scans in 0.58 seconds. The GCC thickness (GCCT) was measured from the inner limiting membrane (ILM) to the outer boundary of the inner plexiform layer (IPL). The built-in software allowed an automated segmentation not only of the total retina from the ILM to the outer border of the retinal pigment epithelium but also of the outer retina from the inner border of the IPL to the outer border of the retinal pigment epithelium.

The recordings of SD-OCT images were done on the same day as the PhNR recordings. The SD-OCT data were analyzed by 2 neuro-ophthalmology specialists (AM, TY). The images of the SD-OCT that had a signal strength index (SSI) less than 45 were excluded and images were also excluded if they included involuntary saccades or blinking artefacts, when an algorithm segmentation error was present, or when the retinal layers were poorly imaged.

Statistical Analyses

Univariate correlation analyses were performed between the PhNRs and the cpRNFLT and the GCCT. Receiver operating characteristic (ROC) curves were created for the W_{ratio}, cpRNFLT, and GCCT in the patients with optic nerve disorders to investigate the ability of these parameters to differentiate eyes with optic nerve disorders from normal control eyes. An ROC curve is a plot of the true-positive rate versus the false-positive rate for all possible cutoff points. The area under the ROC curve (AUC) was used to determine the diagnostic accuracy of each parameter.

All of the statistical analyses were performed using the IBM SPSS Statistics software program (version 23.0, SPSS Japan, Inc, Tokyo, Japan). Differences in diagnostic ability (AUC) was tested for statistical significance using MedCalc statistical software version 18.6 (MedCalc Software Inc, Mariakerke, Belgium). The data are presented as the mean ± SD, and *P* values of <0.05 were taken to be statistically significant.

Declarations

Acknowledgements: We thank Kazuko Haruishi, Nami Mizukami, Yu Manabe, Yuka Kawaguchi, and Misuzu Miyake for performing ophthalmologic examinations on our subjects. We thank Professor Emeritus Duco I. Hamasaki of the Bascom Palmer Eye Institute of the University of Miami (Miami, FL, USA) for critical discussion and final manuscript revision.

Authors' contributions

TY designed the study; SA and KG collected the data; TY, AM, MK and KK interpreted and analyzed the data; YI and JK interpreted the data. TY, KK and MK wrote the manuscript. All authors critically reviewed the manuscript and approved the final manuscript.

Data availability statement

The datasets used and/or analyzed during the current study are available from the corresponding author on reasonable request.

Funding: T. Yamashita, None; M. Kondo, None; K. Kato, None; A. Miki, None; S. Araki, None; K. Goto, None; Y. Ieki, None; J. Kiryu, None.

Conflict of interest: The authors declare that they have no conflict of interest.

Statement of human rights: All procedure performed in this study involving human participants were in accordance with ethical standards of the institutional and/or national research committee and with the 1964 Helsinki declaration and its later amendments or comparable ethical standards.

Statement on the welfare of animals: No animals were used in this study.

References

1 Viswanathan, S., Frishman, L. J., Robson, J. G., Harwerth, R. S. & Smith, E. L., 3rd. The photopic negative response of the macaque electroretinogram: reduction by experimental glaucoma. *Investigative ophthalmology & visual science***40**, 1124-1136 (1999).

2 Rangaswamy, N. V. *et al.* Photopic ERGs in patients with optic neuropathies: comparison with primate ERGs after pharmacologic blockade of inner retina. *Investigative ophthalmology & visual science***45**, 3827-3837, doi:10.1167/iovs.04-0458 (2004).

3 Machida, S. *et al.* Correlation between photopic negative response and retinal nerve fiber layer thickness and optic disc topography in glaucomatous eyes. *Investigative ophthalmology & visual science***49**, 2201-2207, doi:10.1167/iovs.07-0887 (2008).

4 Frishman, L. *et al.* ISCEV extended protocol for the photopic negative response (PhNR) of the full-field electroretinogram. *Documenta ophthalmologica. Advances in ophthalmology***136**, 207-211, doi:10.1007/s10633-018-9638-x (2018).

5 Viswanathan, S., Frishman, L. J., Robson, J. G. & Walters, J. W. The photopic negative response of the flash electroretinogram in primary open angle glaucoma. *Investigative ophthalmology & visual science***42**, 514-522 (2001).

6 Preiser, D., Lagreze, W. A., Bach, M. & Poloschek, C. M. Photopic negative response versus pattern electroretinogram in early glaucoma. *Investigative ophthalmology & visual science***54**, 1182-1191, doi:10.1167/iovs.12-11201 (2013).

7 Machida, S., Gotoh, Y., Tanaka, M. & Tazawa, Y. Predominant loss of the photopic negative response in central retinal artery occlusion. *American journal of ophthalmology***137**, 938-940, doi:10.1016/j.ajo.2003.10.023 (2004).

8 Gotoh, Y., Machida, S. & Tazawa, Y. Selective loss of the photopic negative response in patients with optic nerve atrophy. *Arch Ophthalmol***122**, 341-346, doi:10.1001/archopht.122.3.341 (2004).

9 Wang, J., Cheng, H., Hu, Y. S., Tang, R. A. & Frishman, L. J. The photopic negative response of the flash electroretinogram in multiple sclerosis. *Investigative ophthalmology & visual science***53**, 1315-1323, doi:10.1167/iovs.11-8461 (2012).

10 Tamada, K., Machida, S., Yokoyama, D. & Kurosaka, D. Photopic negative response of full-field and focal macular electroretinograms in patients with optic nerve atrophy. *Japanese journal of ophthalmology***53**, 608-614, doi:10.1007/s10384-009-0731-2 (2009).

11 Maa, A. Y. *et al.* A novel device for accurate and efficient testing for vision-threatening diabetic retinopathy. *Journal of diabetes and its complications***30**, 524-532, doi:10.1016/j.jdiacomp.2015.12.005 (2016).

12 Fukuo, M. *et al.* Screening for diabetic retinopathy using new mydriasis-free, full-field flicker ERG recording device. *Scientific reports***6**, 36591, doi:10.1038/srep36591 (2016).

13 Al-Otaibi, H. *et al.* Validity, Usefulness and Cost of RETeval System for Diabetic Retinopathy Screening. *Translational vision science & technology***6**, 3, doi:10.1167/tvst.6.3.3 (2017).

14 Miyata, R. *et al.* Supernormal Flicker ERGs in Eyes With Central Retinal Vein Occlusion: Clinical Characteristics, Prognosis, and Effects of Anti-VEGF Agent. *Investigative ophthalmology & visual science***59**, 5854-5861, doi:10.1167/iovs.18-25087 (2018).

15 Yasuda, S., Kachi, S., Ueno, S., Piao, C. H. & Terasaki, H. Flicker electroretinograms before and after intravitreal ranibizumab injection in eyes with central retinal vein occlusion. *Acta Ophthalmol***93**, e465-468, doi:10.1111/aos.12674 (2015).

16 Tang, J. *et al.* A Comparison of the RETeval Sensor Strip and DTL Electrode for Recording the Photopic Negative Response. *Translational vision science & technology***7**, 27, doi:10.1167/tvst.7.6.27 (2018).

17 Wu, Z., Hadoux, X., Hui, F., Sarossy, M. G. & Crowston, J. G. Photopic Negative Response Obtained Using a Handheld Electroretinogram Device: Determining the Optimal Measure and Repeatability. *Translational vision science & technology***5**, 8, doi:10.1167/tvst.5.4.8 (2016).

18 Kato, K. *et al.* Factors Affecting Photopic Negative Response Recorded with RETeval System: Study of Young Healthy Subjects. *Translational vision science & technology***9**, 19, doi:10.1167/tvst.9.9.19 (2020).

19 Kirkiewicz, M., Lubiński, W. & Penkala, K. Photopic negative response of full-field electroretinography in patients with different stages of glaucomatous optic neuropathy. *Documenta ophthalmologica. Advances in ophthalmology***132**, 57-65, doi:10.1007/s10633-016-9528-z (2016).

20 López-de-Eguileta, A. & Casado, A. Different follow-up OCT analyses of traumatic optic neuropathy. A case report. *American journal of ophthalmology case reports***20**, 100879, doi:10.1016/j.ajoc.2020.100879 (2020).

21 Kim, G. N. *et al.* Comparison of Lamina Cribrosa Morphology in Normal Tension Glaucoma and Autosomal-Dominant Optic Atrophy. *Investigative ophthalmology & visual science***61**, 9, doi:10.1167/iovs.61.5.9 (2020).

22 Wilsey, L. *et al.* Comparing three different modes of electroretinography in experimental glaucoma: diagnostic performance and correlation to structure. *Documenta ophthalmologica. Advances in ophthalmology***134**, 111-128, doi:10.1007/s10633-017-9578-x (2017).

23 Schweitzer, C. *et al.* Diagnostic Performance of Peripapillary Retinal Nerve Fiber Layer Thickness for Detection of Glaucoma in an Elderly Population: The ALIENOR Study. *Investigative ophthalmology & visual science***57**, 5882-5891, doi:10.1167/iovs.16-20104 (2016).

24 North, R. V., Jones, A. L., Drasdo, N., Wild, J. M. & Morgan, J. E. Electrophysiological evidence of early functional damage in glaucoma and ocular hypertension. *Investigative ophthalmology & visual science***51**, 1216-1222, doi:10.1167/iovs.09-3409 (2010).

25 Machida, S. *et al.* Comparison of photopic negative response of full-field and focal electroretinograms in detecting glaucomatous eyes. *Journal of ophthalmology***2011**, doi:10.1155/2011/564131 (2011).

26 Bertuzzi, F. *et al.* Diagnostic validity of optic disc and retinal nerve fiber layer evaluations in detecting structural changes after optic neuritis. *Ophthalmology***117**, 1256-1264.e1251, doi:10.1016/j.ophtha.2010.02.024 (2010).

27 Moon, Y., Song, M. K., Shin, J. W. & Lim, H. T. Optical Coherence Tomography Angiography Characteristics and Predictors of Visual Outcomes in Patients With Acute and Chronic Nonarteritic Anterior Ischemic Optic Neuropathy. *Journal of neuro-ophthalmology : the official journal of the North American Neuro-Ophthalmology Society***41**, e440-e450, doi:10.1097/wno.0000000000001102 (2021).

28 Akaishi, T. *et al.* Repeated follow-up of AQP4-IgG titer by cell-based assay in neuromyelitis optica spectrum disorders (NMOSD). *Journal of the neurological sciences***410**, 116671, doi:10.1016/j.jns.2020.116671 (2020).

29 Diao, T. *et al.* Comparison of Machine Learning Approaches to Improve Diagnosis of Optic Neuropathy Using Photopic Negative Response Measured Using a Handheld Device. *Frontiers in medicine***8**, 771713, doi:10.3389/fmed.2021.771713 (2021).

30 Mortlock, K. E., Binns, A. M., Aldebasi, Y. H. & North, R. V. Inter-subject, inter-ocular and inter-session repeatability of the photopic negative response of the electroretinogram recorded using DTL and skin electrodes. *Documenta ophthalmologica. Advances in ophthalmology***121**, 123-134, doi:10.1007/s10633-010-9239-9 (2010).

Figures

Figure 1

Representative cases of optic nerve disorders and control subjects.

In each case, a photograph of the optic nerve papilla, temporal-superior-nasal-inferior-temporal (TSNIT) graph of circumpapillary retinal nerve fiber thickness (cpRNFLT) and PhNR waveform were shown. The solid black line in the TSNIT graph represents the patient's cpRNFLT.

Top left: Normal control subjects. Full-field ERGs show negative wave immediately after the b-wave (red arrow).

Top right: Acute phase of non-arteritic ischemic optic neuropathy. Fundus photograph shows segmental optic disc swelling with flame-shaped hemorrhage. The PhNR is severely attenuated.

Bottom left: Chronic phase of non-arteritic ischemic optic neuropathy. Fundus photograph shows mild atrophy of the optic disk. PhNR is severely attenuated.

Bottom right: Traumatic optic neuropathy. Fundus photograph shows pallor of the optic disk. The PhNR is severely attenuated.

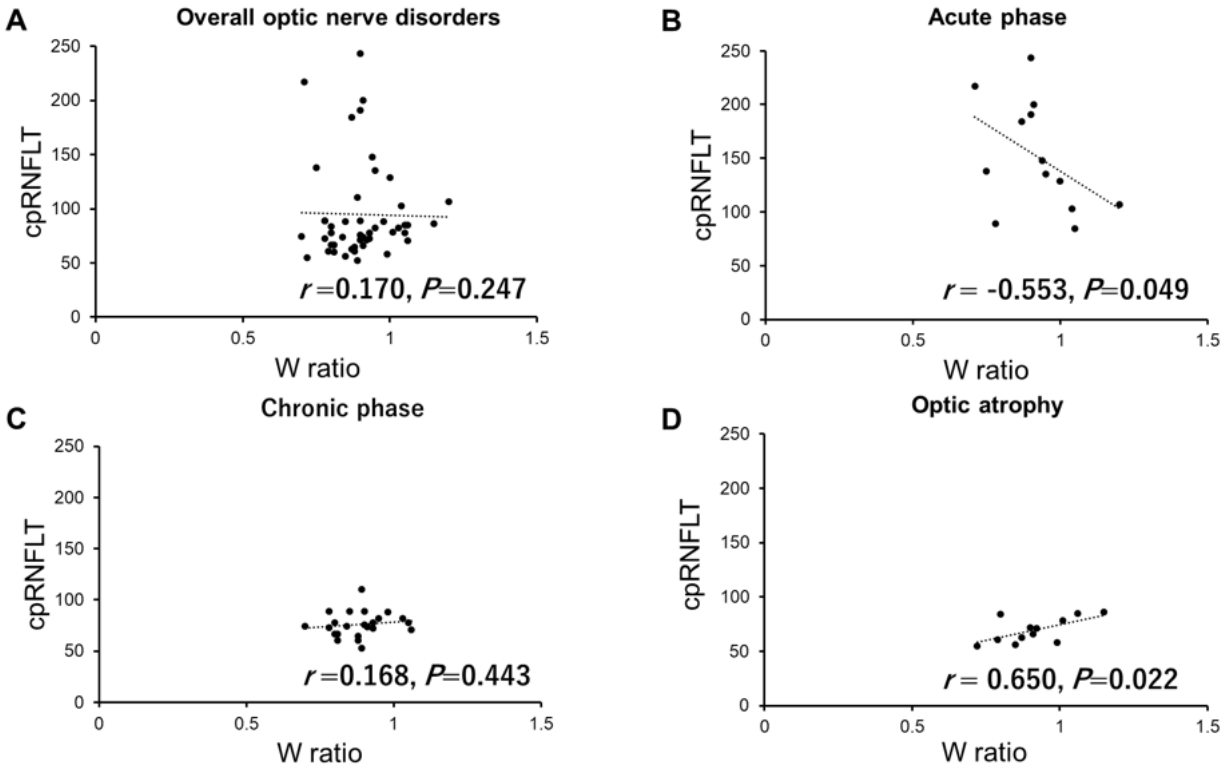

Figure 2

Graph showing the relationship between the W_{ratio} and cpRNFLT in optic nerve disorders.

Scatterplots of all of the cases of optic nerve disorders (A), acute phase of optic neuritis, and ischemic optic neuropathy **(B)**, chronic phase of optic neuritis or ischemic optic neuropathy **(C)**, dominant optic neuropathy or traumatic optic atrophy versus cpRNFLT **(D)**.

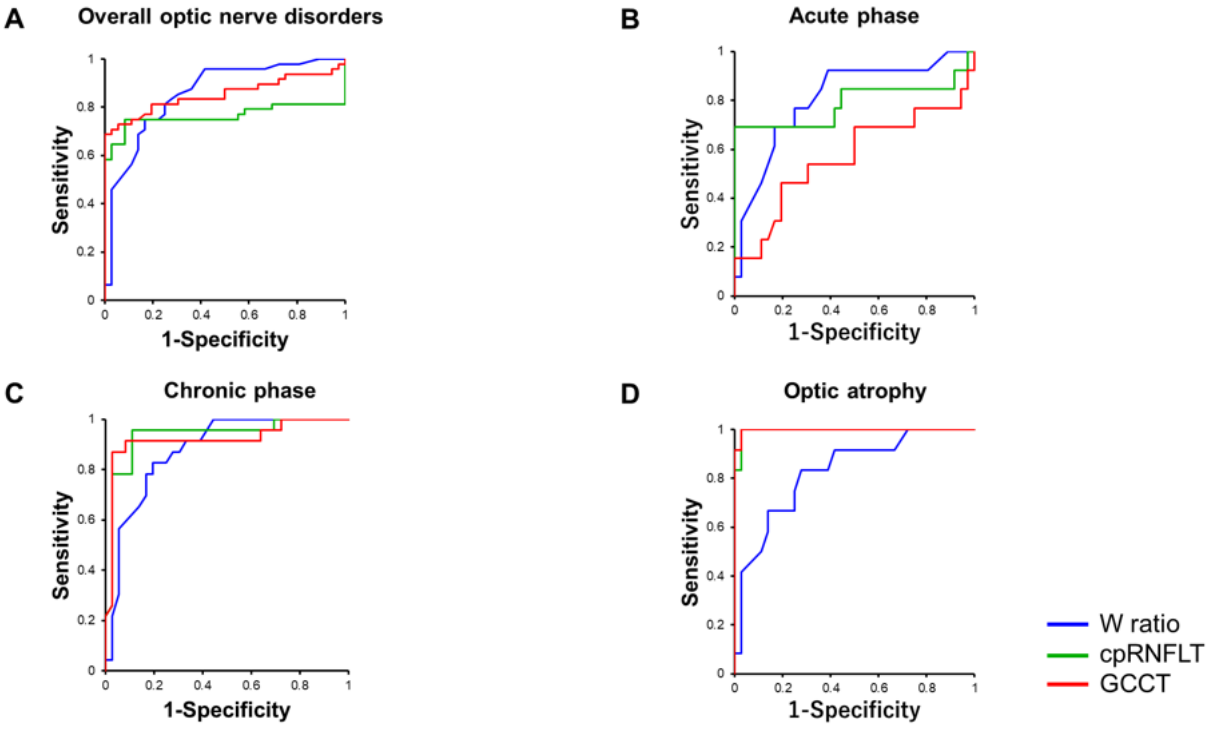

Figure 3

Receiver operating characteristic (ROC) curves for detecting optic nerve disorders.

Blue, green, and red lines show the ROC curves for detecting optic nerve disorders using the W_{ratio}, cpRNFLT and GCCT as indices respectively.

(A). Overall optic nerve disorders, **(B).** Acute phase of optic neuritis or ischemic optic neuropathy, **(C)** chronic phase of optic neuritis or optic neuropathy, **(D)** hereditary or traumatic optic atrophy.

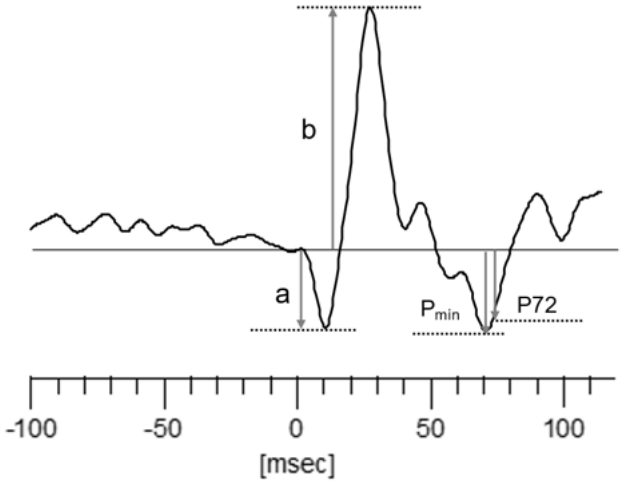

P72 : The negative voltage at 72msec

P_{min} : The negative trough voltage following of the b -wave

P ratio = -P72/b

W ratio= $(b-P_{min})/(b-a)$

Figure 4

Illustration of the methods to measure various components of the ERG waveform.

Arrows represent the amplitude of each parameter. The a-wave amplitude was measured from the pre-stimulus baseline to the first negative trough (a). The b-wave amplitude was measured from the a-wave trough to the positive peak (b-a). The P72 amplitude was measured at 72 ms after the stimulus onset, and the amplitude of P_{min} was measured at the negative trough following the b-wave. The calculation of P_{ratio} and W_{ratio} was done as shown in the figure.